

## LETTERS

# Optical rogue waves

D. R. Solli<sup>1</sup>, C. Ropers<sup>1,2</sup>, P. Koonath<sup>1</sup> & B. Jalali<sup>1</sup>

Recent observations show that the probability of encountering an extremely large rogue wave in the open ocean is much larger than expected from ordinary wave-amplitude statistics<sup>1–3</sup>. Although considerable effort has been directed towards understanding the physics behind these mysterious and potentially destructive events, the complete picture remains uncertain. Furthermore, rogue waves have not yet been observed in other physical systems. Here, we introduce the concept of optical rogue waves, a counterpart of the infamous rare water waves. Using a new real-time detection technique, we study a system that exposes extremely steep, large waves as rare outcomes from an almost identically prepared initial population of waves. Specifically, we report the observation of rogue waves in an optical system, based on a microstructured optical fibre, near the threshold of soliton-fission supercontinuum generation<sup>4,5</sup>—a noise-sensitive<sup>5–7</sup> nonlinear process in which extremely broadband radiation is generated from a narrowband input<sup>8</sup>. We model the generation of these rogue waves using the generalized nonlinear Schrödinger equation<sup>9</sup> and demonstrate that they arise infrequently from initially smooth pulses owing to power transfer seeded by a small noise perturbation.

For centuries, seafarers have told tales of giant waves that can appear without warning on the high seas. These mountainous waves were said to be capable of destroying a vessel or swallowing it beneath the surface, and then disappearing without the slightest trace. Until recently, these tales were thought to be mythical. In the mid-1990s, however, freak waves proved very real when recorded for the first time by scientific measurements during an encounter at the Draupner oil platform in the North Sea<sup>3</sup>. Although they are elusive and intrinsically difficult to monitor because of their fleeting existences, satellite surveillance has confirmed that rogue waves roam the open oceans, occasionally encountering a ship or sea platform, sometimes with devastating results<sup>1</sup>. It is now believed that a number of infamous maritime disasters were caused by such encounters<sup>10</sup>.

The unusual statistics of rogue waves represent one of their defining characteristics. Conventional models of ocean waves indicate that the probability of observing large waves should diminish extremely rapidly with wave height, suggesting that the likelihood of observing even a single freak wave in hundreds of years should be essentially non-existent. In reality, however, ocean waves appear to follow ‘L-shaped’ statistics: most waves have small amplitudes, but extreme outliers also occur much more frequently than expected in ordinary (for example, gaussian or Rayleigh) wave statistics<sup>11–13</sup>.

It is likely that more than one process can produce occasional extreme waves with small but non-negligible probability<sup>14,15</sup>. Possible mechanisms that have been suggested to explain oceanic rogue waves include effects such as nonlinear focusing via modulation instability in one dimension<sup>16,17</sup> and in two-dimensional crossings<sup>18,19</sup>, nonlinear spectral instability<sup>20</sup>, focusing with caustic currents<sup>21</sup> and anomalous wind excitation<sup>12</sup>. Nonlinear mechanisms have attracted particular attention because they possess the requisite extreme sensitivity to initial conditions.

Although the physics behind rogue waves is still under investigation, observations indicate that they have unusually steep, solitary or tightly grouped profiles, which appear like “walls of water”<sup>10</sup>. These features imply that rogue waves have relatively broadband frequency content compared with normal waves, and also suggest a possible connection with solitons—solitary waves, first observed by J. S. Russell in the nineteenth century, that propagate without spreading in water because of a balance between dispersion and nonlinearity. As rogue waves are exceedingly difficult to study directly, the relationship between rogue waves and solitons has not yet been definitively established, but it is believed that they are connected.

So far, the study of rogue waves in the scientific literature has focused on hydrodynamic studies and experiments. Intriguingly, there are other physical systems that possess similar nonlinear characteristics and may also support rogue waves. Here we report the observation and numerical modelling of optical rogue waves in a system based on probabilistic supercontinuum generation in a highly nonlinear microstructured optical fibre. We coin the term ‘optical rogue waves’ based on striking phenomenological and physical similarities between the extreme events of this optical system and oceanic rogue waves.

Supercontinuum generation has received a great deal of attention in recent years for its complex physics and wealth of potential applications<sup>5,8</sup>. An extremely broadband supercontinuum source can be created by launching intense seed pulses into a nonlinear fibre at or near its zero-dispersion wavelength<sup>22</sup>. In this situation, supercontinuum production involves generation of high-order solitons—the optical counterparts of Russell’s solitary water waves—which fission into redshifted solitonic and blueshifted non-solitonic components at different frequencies<sup>4,5</sup>. The solitonic pulses shift further towards the red as they propagate through the nonlinear medium because of the Raman-induced self-frequency shift<sup>9</sup>. Interestingly, frequency downshifting effects are also known to occur in water wave propagation. It has been noted that the aforementioned Raman self-frequency shift represents an analogous effect in optics<sup>23</sup>. The nonlinear processes responsible for supercontinuum generation amplify the noise present in the initial laser pulse<sup>6,7</sup>. Especially for long pulses and continuous-wave input radiation, modulation instability—an incoherent nonlinear wave-mixing process—broadens the spectrum from seed noise in the initial stages of propagation and, as a result, the output spectrum is highly sensitive to the initial conditions<sup>24,25</sup>.

A critical challenge in observing optical rogue waves is the lack of real-time instruments that can capture a large number of very short random events in a single shot. To solve this problem, we use a wavelength-to-time transformation technique inspired by the concept of photonic time-stretch analog-to-digital conversion<sup>26</sup>. In the present technique, group-velocity dispersion (GVD) is used to stretch the waves temporally so that many thousands of random ultra-short events can be captured in real time. A different single-shot technique has been used to study isolated supercontinuum pulses<sup>27</sup>; however, the real-time capture of a large number of random

<sup>1</sup>Department of Electrical Engineering, University of California, Los Angeles 90095, USA. <sup>2</sup>Max Born Institute for Nonlinear Optics and Short Pulse Spectroscopy, D-12489 Berlin, Germany.

events has not been reported. Using the present method, a small but statistically significant fraction of extreme waves can be discerned from a large number of ordinary events, permitting the first observation of optical rogue waves.

The supercontinuum radiation used in our experiments is generated by sending picosecond seed pulses at 1,064 nm through a length of highly nonlinear microstructured optical fibre with matched zero-dispersion wavelength. The output is red-pass filtered at 1,450 nm and stretched as described above so that many thousands of events can be captured with high resolution in a single-shot measurement. A schematic of the experimental apparatus is displayed in Fig. 1 and additional details are provided in the Methods Summary.

Using this setup, we acquire large sets of pulses in real time for very low seed pulse power levels—power levels below the threshold required to produce appreciable supercontinuum. We find that the pulse-height distributions are sharply peaked with a well-defined mean, but contrary to expectation, rare events with far greater intensities also appear. In Fig. 1, we show representative single-shot time traces and histograms for three different low power levels. In these traces, the vast majority of events are concentrated in a small number of bins and are so weak that they are buried beneath the noise floor of the measurement process; however, the most extreme ones reach intensities at least 30–40 times the average. The histograms display a clear L-shaped profile, with extreme events occurring rarely, yet

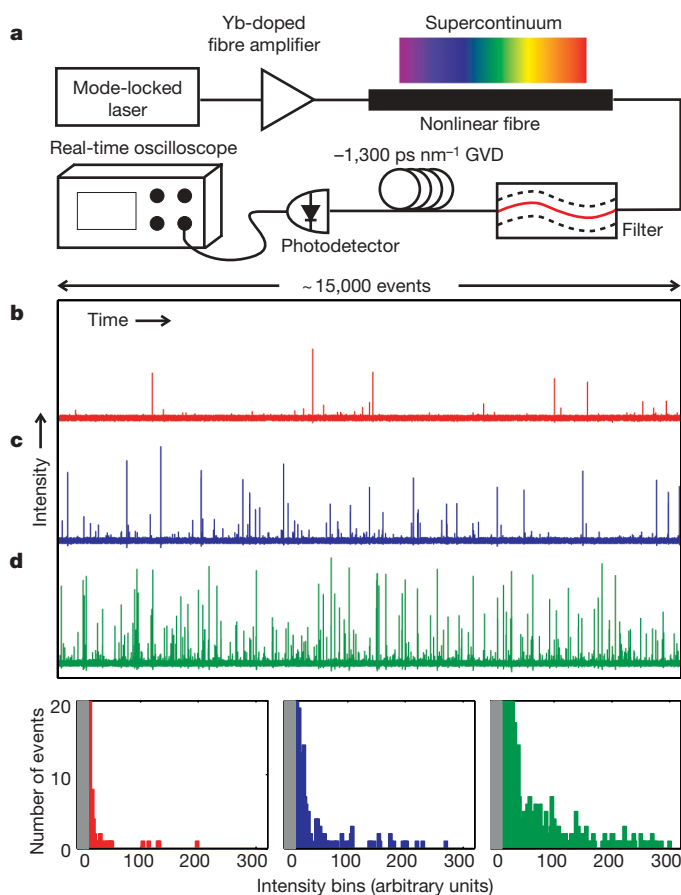


**Figure 1 | Experimental observation of optical rogue waves.** **a**, Schematic of experimental apparatus. **b–d**, Single-shot time traces containing roughly 15,000 pulses each and associated histograms (bottom of figure: left, **b**; middle, **c**; right, **d**) for average power levels 0.8  $\mu\text{W}$  (red), 3.2  $\mu\text{W}$  (blue) and 12.8  $\mu\text{W}$  (green), respectively. The grey shaded area in each histogram demarcates the noise floor of the measurement process. In each measurement, the vast majority of events (>99.5% for the lowest power) are buried in this low intensity range, and the rogue events reach intensities of at least 30–40 times the average value. These distributions are very different from those encountered in most stochastic processes.

much more frequently than expected based on the relatively narrow distribution of typical events.

Because the red-pass filter transmits only a spectral region that is nearly dark in the vast majority of events, the rare events clearly have extremely broadband, frequency-downshifted spectral content. The data also show that the frequency of occurrence of the rogue events increases with the average power, but the maximum height of a freak pulse remains relatively constant. These features indicate that the extreme events are sporadic, single solitons.

The nonlinear Schrödinger equation (NLSE) models soliton dynamics and has also been used to study hydrodynamic rogue waves generated by nonlinear energy transfer in the open ocean<sup>16–19</sup>. As the NLSE also describes optical pulse propagation in nonlinear media, it is certainly plausible that this equation could predict optical rogue waves. We investigate this numerically using the generalized NLSE (neglecting absorption), which is widely used for broadband optical pulse propagation in nonlinear fibres<sup>9</sup>. The generalized NLSE incorporates dispersion and the Kerr nonlinearity, as well as approximations for self-steepening and the vibrational Raman response of the medium. This equation has been successfully used to model supercontinuum generation in the presence of noise<sup>28,29</sup> and, as we demonstrate here, is capable of qualitatively explaining our experimental results. In anticipation of broadband application, we include several higher orders of dispersion in the nonlinear fibre, which we calculated from the manufacturer's test data (see Methods). Similarly, higher-order dispersion has also been used to extend the validity of the NLSE for broadband calculations in hydrodynamics<sup>30</sup>.

As expected, the present model shows that a high-power, smooth input pulse ejects multiple redshifted solitons and blueshifted non-solitonic components, and a tiny amount of input noise varies their spectral content<sup>5,25</sup>. On the other hand, for low power levels, the spectral content of the pulse broadens, but no sharp soliton is shed. In this case, the situation changes markedly when a tiny amount of noise is added. This perturbation is amplified by nonlinear interactions including modulation instability, which dramatically lowers the soliton-fission threshold and permits unpredictable freak events to develop. Interestingly, the hydrodynamic equivalent—the Benjamin–Feir modulation instability—is also thought to initiate hydrodynamic rogue waves<sup>16–19</sup>. This instability spreads spectral content from a narrow bandwidth to a broader range in the initial stages of water wave propagation, just as it does in this optical system.

We include a stochastic perturbation in our simulations by adding to the initial pulse envelope a small amount of bandwidth-restricted random noise with amplitude proportional to the instantaneous field strength. We then solve the NLSE repeatedly for a large number of independent events. For a small fraction of events, the spectrum becomes exceptionally broad with a clear redshifted solitonic shoulder.

Figure 2a shows the time trace and histogram of peak heights for a trial of 1,000 events after red-pass filtering each output pulse at the start of the solitonic shoulder illustrated in Fig. 2b. Clearly, the histogram of heights is sharply peaked but has extended tails, as observed in the experiment, and the distribution contains rogue events more than 50 times as large as the mean. The same rogue events are identified regardless of where the filter is located within the smooth solitonic shoulder and can also be identified from the complementary non-solitonic blue side of the spectrum.

The rogue pulses have exceptionally steep leading and trailing edges compared with the initial pulses and the typical events, as shown in Fig. 2c. The wide bandwidth and abrupt temporal profile of an optical rogue wave is also highlighted in Fig. 3 where the power is displayed as a function of both wavelength and time using a short-time Fourier transform. Because there are no apparent features in the perturbations that lead to the development of the rogue events, their appearance seems unpredictable.

To pinpoint the underlying feature of the noise that produces rogue waves, we have closely analysed the temporal and spectral properties of the initial conditions. Examining the correlations

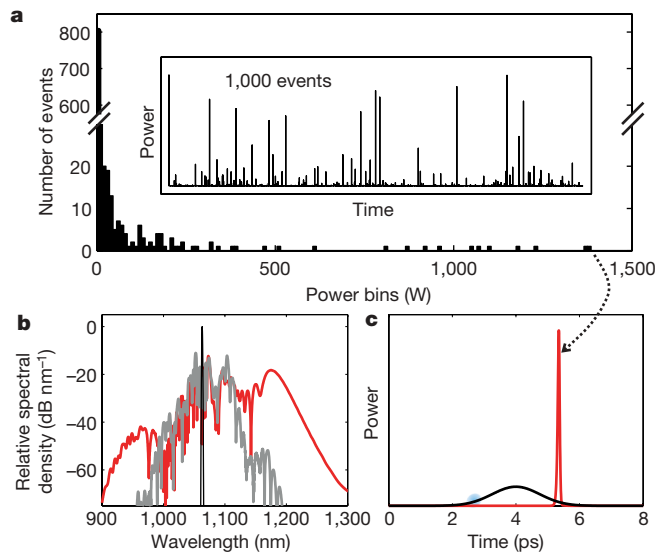


**Figure 2 | Simulation of optical rogue waves using the generalized nonlinear Schrödinger equation.** **a**, The time trace and histogram of 1,000 events with red-pass filtering from 1,155 nm. The initial (seed) pulses have width 3 ps, peak power 150 W, fractional noise 0.1%, and noise bandwidth 50 THz. The vertical axis of the histogram contains a scale break to make it easier to see the disparity between the most common events at low peak power and the rogue events at high peak power. **b**, The complete relative spectral densities of the initial pulse (black line), a typical event (grey line) and the rare event shown in **c** (red line). **c**, The markedly different temporal profiles of the seed pulse and the rare event indicated in the histogram. The typical events from the histogram are so tiny that they are not visible on this linear power scale. The shaded blue region on the seed pulse delineates the time window that is highly sensitive to perturbation.

between the initial conditions and their respective output waveforms, we find that if the random noise happens to contain energy with a frequency shift of about 8 THz within a 0.5-ps window centred about 1.4 ps before the pulse peak (Fig. 2c), a rogue wave is born. Noise at this particular frequency shift and on a leading portion of the pulse envelope efficiently seeds modulation instability, reshaping the pulse to hasten its breakup. The output wave height correlates in a highly nonlinear way with this specific aspect of the initial conditions. Thus, the normal statistics of the input noise are transformed into an extremely skewed, L-shaped distribution of output wave heights. Further study is needed to explain precisely why the pulse is so highly sensitive to these particular noise parameters. Nevertheless, the specific feature we have identified in the initial conditions offers some predictive power for optical rogue waves, and may offer clues to the oceanic phenomenon.

The rogue waves have a number of other intriguing properties warranting further study. For example, they propagate without noticeable broadening for some time, but have a finite, seemingly unpredictable lifetime before they suddenly collapse owing to cumulative effects of Raman scattering. This scattering seeded by noise dissipates energy or otherwise perturbs the soliton pulse beyond the critical threshold for its survival<sup>9</sup>. The decay parallels the unpredictable lifetimes of oceanic rogue waves. The rogue optical solitons are also able to absorb energy from other wavepackets they pass through, which causes them to grow in amplitude, but appears to reduce their lifetime. A similar effect may help to explain the development of especially large rogues in the ocean.

In conclusion, we have observed extreme soliton-like pulses that are the optical equivalent of oceanic rogue waves. These rare optical events possess the hallmark phenomenological features of oceanic rogue waves—they are extremely large and seemingly unpredictable, follow unusual L-shaped statistics, occur in a nonlinear medium, and are broadband and temporally steep compared with typical events.

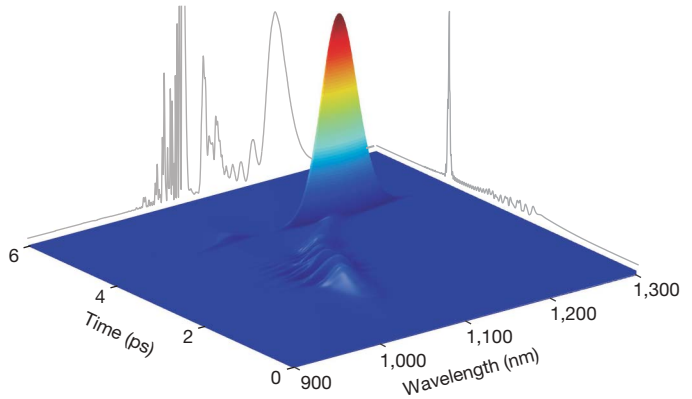


**Figure 3 | Time-wavelength profile of an optical rogue wave obtained from a short-time Fourier transform.** The optical wave has broad bandwidth and has extremely steep slopes in the time domain compared with the typical events. It appears as a ‘wall of light’ analogous to the ‘wall of water’ description of oceanic rogue waves. The rogue wave travels a curved path in time-wavelength space because of the Raman self-frequency shift and group velocity dispersion, separating from non-solitonic fragments and remnants of the seed pulse at shorter wavelengths. The grey traces show the full time structure and spectrum of the rogue wave. The spectrum contains sharp spectral features that are temporally broad and, thus, do not reach large peak power levels and do not appear prominently in the short-time Fourier transform.

On a physical level, the similarities also abound, with modulation instability, solitons, frequency downshifting and higher-order dispersion as striking points of connection. Intriguingly, the rogue waves of both systems can be modelled with the nonlinear Schrödinger equation. Although the parameters that characterize this optical system are of course very different from those describing waves on the open ocean, the rogue waves generated in the two cases bear some remarkable similarities.

## METHODS SUMMARY

Our supercontinuum source consists of a master oscillator, a fibre amplifier, and a 15-m length of highly nonlinear microstructured fibre whose zero-dispersion point matches the seed wavelength. The master oscillator is a mode-locked ytterbium-doped fibre laser producing picosecond pulses at about 1,064 nm with a repetition rate of 20 MHz. The output pulses are amplified to a desired level in a large-mode-area ytterbium-doped-fibre amplifier. This amplification process yields chirped pulses of ~5-nm bandwidth and a few picoseconds temporal width.

The wavelength-to-time transformation for real-time detection is accomplished using a highly dispersive optical fibre producing about  $-1,300 \text{ ps nm}^{-1}$  of GVD over the wavelength range of interest. Because the supercontinuum output is red-pass filtered with a cut-on wavelength of 1,450 nm, adjacent pulses do not overlap in time after being stretched. The GVD-stretched signal is then fed to a fast photodetector and captured by a real-time 20-gigasample-per-second oscilloscope, which records sequences of ~15,000 pulses with high temporal resolution in a single-shot measurement.

The detection of rogue events is insensitive to the filter window, so the specific choice of the red-pass cut-on wavelength is not critical. The soliton shoulder shown in Fig. 2b is smooth and extends to very long wavelengths, so a freak soliton can be detected by examining any section of this extended region. Because of experimental constraints, we limit the measurements to the long-wavelength tail of the soliton shoulder, whereas, in the simulations, it is instructive to capture the entire soliton spectrum. The simulations show that it is acceptable to detect the rogue events experimentally by their red tails because the same rogue events are identified no matter where the filter is located throughout this spectral region.

**Full Methods** and any associated references are available in the online version of the paper at [www.nature.com/nature](http://www.nature.com/nature).

Received 22 February; accepted 11 October 2007.

- Hopkin, M. Sea snapshots will map frequency of freak waves. *Nature* **430**, 492 (2004).

2. Perkins, S. Dashing rogues: freak ocean waves pose threat to ships, deep-sea oil platforms. *Science News* **170**, 328–329 (2006).
3. Broad, W. J. Rogue giants at sea. *The New York Times* (July 11, 2006).
4. Herrmann, J. *et al.* Experimental evidence for supercontinuum generation by fission of higher-order solitons in photonic fibers. *Phys. Rev. Lett.* **88**, 173901 (2002).
5. Dudley, J. M., Genty, G. & Coen, S. Supercontinuum generation in photonic crystal fiber. *Rev. Mod. Phys.* **78**, 1135–1184 (2006).
6. Corwin, K. L. *et al.* Fundamental noise limitations to supercontinuum generation in microstructure fiber. *Phys. Rev. Lett.* **90**, 113904 (2003).
7. Gaeta, A. L. Nonlinear propagation and continuum generation in microstructured optical fibers. *Opt. Lett.* **27**, 924–926 (2002).
8. Alfano, R. R. The ultimate white light. *Sci. Am.* **295**, 87–93 (2006).
9. Agrawal, G. P. *Nonlinear Fiber Optics* 3rd edn (Academic, San Diego, 2001).
10. Kharif, C. & Pelinovsky, E. Physical mechanisms of the rogue wave phenomenon. *Eur. J. Mech. B Fluids* **22**, 603–634 (2003).
11. Dean, R. G. & in. *Water Wave Kinematics* (eds Tørum, A. & Gudmestad, O. T.) 609–612 (Kluwer, Amsterdam, 1990).
12. Muller, P., Garrett, C. & Osborne, A. Rogue waves. *Oceanography* **18**, 66–75 (2005).
13. Walker, D. A. G., Taylor, P. H. & Taylor, R. E. The shape of large surface waves on the open sea and the Draupner New Year wave. *Appl. Ocean. Res.* **26**, 73–83 (2004).
14. Dysthe, K., Socquet-Juglard, H., Trulsen, K., Krogstad, H. E. & Liu, J. "Freak" waves and large-scale simulations of surface gravity waves. *Rogue Waves, Proc. 14th 'Aha Huliko'a Hawaiian Winter Workshop* 91–99 (Univ. Hawaii, Honolulu, 2005).
15. Liu, P. C. & MacHutchon, K. R. Are there different kinds of rogue waves? *Proc. OMAE2006, 25th Int. Conf. Offshore Mechanics and Arctic Engineering*, Paper No. 92619, 1–6 (American Society of Mechanical Engineers, New York, 2006).
16. Henderson, K. L., Peregrine, K. L. & Dold, J. W. Unsteady water wave modulations: fully nonlinear solutions and comparison with the nonlinear Schrödinger equation. *Wave Motion* **29**, 341–361 (1999).
17. Onorato, M., Osborne, A. R., Serio, M. & Bertone, S. Freak waves in random oceanic sea states. *Phys. Rev. Lett.* **86**, 5831–5834 (2001).
18. Onorato, M., Osborne, A. R. & Serio, M. Modulational instability in crossing sea states: A possible mechanism for the formation of freak waves. *Phys. Rev. Lett.* **96**, 014503 (2006).
19. Shukla, P. K., Kourakis, I., Eliasson, B., Marklund, M. & Stenflo, L. Instability and evolution of nonlinearly interacting water waves. *Phys. Rev. Lett.* **97**, 094501 (2006).
20. Janssen, P. A. E. M. Nonlinear four-wave interactions and freak waves. *J. Phys. Oceanogr.* **33**, 863–884 (2003).
21. White, B. S. & Fornberg, B. On the chance of freak waves at sea. *J. Fluid Mech.* **355**, 113–138 (1998).
22. Ranka, J. K., Windeler, R. S. & Stentz, A. J. Visible continuum generation in air–silica microstructure optical fibers with anomalous dispersion at 800 nm. *Opt. Lett.* **25**, 25–27 (2000).
23. Segur, H. *et al.* Stabilizing the Benjamin–Feir instability. *J. Fluid Mech.* **539**, 229–271 (2005).
24. Islam, M. N. *et al.* Femtosecond distributed soliton spectrum in fibers. *J. Opt. Soc. Am. B* **6**, 1149–1158 (1989).
25. Kutz, J. N., Lyngå, C. & Eggleton, B. J. Enhanced supercontinuum generation through dispersion-management. *Opt. Express* **13**, 3989–3998 (2005).
26. Han, Y., Boyraz, O. & Jalali, B. Tera-sample per second real-time waveform digitizer. *Appl. Phys. Lett.* **87**, 241116 (2005).
27. Gu, X. *et al.* Frequency-resolved optical gating and single-shot spectral measurements reveal fine structure in microstructure-fiber continuum. *Opt. Lett.* **27**, 1174–1176 (2002).
28. Nakazawa, M., Kubota, H. & Tamura, K. Random evolution and coherence degradation of a high-order optical soliton train in the presence of noise. *Opt. Lett.* **24**, 318–320 (1999).
29. Boyraz, O., Kim, J., Islam, M. N., Coppinger, F. & Jalali, B. 10 Gb/s multiple wavelength, coherent short pulse source based on spectral carving of supercontinuum generated in fibers. *J. Lightwave Technol.* **18**, 2167–2175 (2000).
30. Trulsen, K. & Dysthe, K. B. A modified nonlinear Schrödinger equation for broader bandwidth gravity waves on deep water. *Wave Motion* **24**, 281–289 (1996).

**Author Information** Reprints and permissions information is available at [www.nature.com/reprints](http://www.nature.com/reprints). Correspondence and requests for materials should be addressed to D.R.S. ([solli@ucla.edu](mailto:solli@ucla.edu)).

## METHODS

Our simulations are based on the nonlinear Schrödinger equation (NLSE), which governs the propagation of optical pulses and has been widely used to model supercontinuum generation in optical fibres. The equation describes the evolution of the slowly varying electric field envelope,  $A(z,t)$ , in the presence of temporal dispersion and nonlinearity. In its generalized form, the NLSE accounts for dispersion as well as both the electronic (instantaneous) and vibrational (delayed) nonlinearities in silica glass. For many applications, it is sufficient to use approximations for these nonlinearities that are physically intuitive and efficient for numerical computations using the well-known split-step method. Relative to a reference frame co-moving with the optical pulse, this form of the equation can be expressed as

$$\frac{\partial A}{\partial z} - i \sum_{m=2} \frac{i^m \beta_m}{m!} \frac{\partial^m A}{\partial t^m} = i\gamma \left[ |A|^2 A + \frac{i}{\omega_0} \frac{\partial}{\partial t} (|A|^2 A) - T_R A \frac{\partial |A|^2}{\partial t} \right]$$

where  $\beta_m$  are values that characterize the fibre dispersion,  $\gamma$  is the nonlinear coefficient of the fibre,  $\omega_0$  is the central carrier frequency of the field, and  $T_R$  is a parameter that characterizes the delayed nonlinear response of silica fibre<sup>9</sup>. The bracketed terms on the right-hand side of the equation describe the Kerr nonlinearity, self-steepening and the vibrational Raman response of the medium, respectively. For completeness, we include the self-steepening term in our simulations, but we have found that it is not required for rogue wave generation. The Kerr term produces self-phase modulation, and the Raman term causes frequency downshifting of the carrier wave.

This form of the NLSE has been successfully used in the literature to model supercontinuum generation in the presence of noise and is capable of qualitatively explaining our experimental results. In our calculations, we include dispersion up to sixth order, which we calculated from the manufacturer's test data (see Crystal Fibre NL-5.0-1065 for fibre specifications). Operating at the zero dispersion wavelength of the fibre, we use the dispersion parameters  $\beta_2 \approx 0$ ,  $\beta_3 \approx 7.67 \times 10^{-5} \text{ ps}^3 \text{ m}^{-1}$ ,  $\beta_4 \approx -1.37 \times 10^{-7} \text{ ps}^4 \text{ m}^{-1}$ ,  $\beta_5 \approx 3.61 \times 10^{-10} \text{ ps}^5 \text{ m}^{-1}$ , and  $\beta_6 \approx 5.06 \times 10^{-13} \text{ ps}^6 \text{ m}^{-1}$ . The nonlinear coefficient and the Raman response parameter are given by  $\gamma = 11 \text{ W}^{-1} \text{ km}^{-1}$  and  $T_R = 5 \text{ fs}$ . These numbers model the experimental situation, but we find that the NLSE can also produce rogue wave solutions with other values of the parameters.

To generate rogue waves, we perturb the input pulse by adding a very small amount of amplitude noise directly to its temporal envelope. Specifically, at each point in time, a small random number is added to the input field envelope. The noise amplitude at each point is proportional to the instantaneous amplitude of the pulse. The peak power of the unperturbed pulse is chosen to be small enough that the pulse will not break up without the noise perturbation. We then apply a frequency bandpass filter to limit the input noise to a relatively narrow bandwidth around the seed wavelength, sufficient to mimic the optical noise bandwidth of the input field in the experiment. The specific noise amplitude and peak power of the pulse are not critical, but influence the rogue wave generation rate. Noise amplitudes of the order of 0.1% of the pulse amplitude or even significantly less are adequate to observe a rare, but reasonable generation rate. Although we include noise in this particular way, this specific form is not required to create rogue waves—other perturbations produce similar results. This particular form of noise serves as a conceptually simple perturbation that qualitatively accounts for our experimental results. When we solve the NLSE repeatedly given these conditions, rogue waves are produced as statistically rare events from members of an initial population that are nearly indistinguishable.